Author for correspondence:
Patrícia Rita
e-mail: patricia.rita@fau.de

THE ROYAL SOCIETY PUBLISHING

Mechanisms and drivers of belemnite body-size dynamics across the Pliensbachian–Toarcian crisis

Patrícia Rita[1,2], Paulina Nätscher[1], Luís V. Duarte[2,3], Robert Weis[4] and Kenneth De Baets[1]

[1]Geozentrum Nordbayern, Friedrich-Alexander-Universität Erlangen-Nürnberg, Erlangen 91054, Germany
[2]MARE (Marine and Environmental Sciences Centre), 3004-517 Coimbra, Portugal
[3]Department of Earth Sciences, University of Coimbra, 3070-790 Coimbra, Portugal
[4]National Museum of Natural History Luxembourg, Department of Palaeontology, 2160 Luxembourg, Luxembourg

(iD) PR, 0000-0002-7839-2433; KDB, 0000-0002-1651-321X

Body-size reduction is considered an important response to current climate warming and has been observed during past biotic crises, including the Pliensbachian–Toarcian crisis, a second-order mass extinction. However, in fossil cephalopod studies, the mechanisms and their potential link with climate are rarely investigated and palaeobiological scales of organization are not usually differentiated. Here, we hypothesize that belemnites reduce their adult size across the Pliensbachian–Toarcian boundary warming event. Belemnite body-size dynamics across the Pliensbachian–Toarcian boundary in the Peniche section (Lusitanian Basin, Portugal) were analysed based on the newly collected field data. We disentangle the mechanisms and the environmental drivers of the size fluctuations observed from the individual to the assemblage scale. Despite the lack of a major taxonomic turnover, a 40% decrease in rostrum volume is observed across the Pliensbachian–Toarcian boundary, before the Toarcian Oceanic Anoxic Event where belemnites go locally extinct. The pattern is mainly driven by a reduction in adult size of the two dominant species, *Pseudohastites longiformis* and *Passaloteuthis bisulcata*. Belemnite-size distribution is best correlated with fluctuations in a palaeotemperature proxy (stable oxygen isotopes); however, potential indirect effects of volcanism and carbon cycle perturbations may also play a role. This highlights the complex interplay between environmental stressors (warming, deoxygenation, nutrient input) and biotic variables (productivity, competition, migration) associated with these hyperthermal events in driving belemnite body-size.

1. Introduction

Body-size is a key feature of any organism, reflecting its physiology, ecology and evolutionary history, across multiple scales of biological organization [1]. Body-size reduction has been considered the third universal response to global warming, after changes in phenology and species distribution [2–4]. However, disentangling body-size responses to warming might not be straightforward due to the interactions between biotic and abiotic factors involved in climate warming episodes [5,6], even in the Jurassic, when additional factors, like human activities, were absent [6,7]. Many factors during climate warming (increased temperature, decreased oxygenation and ocean acidification) are likely to work in synergy in leading to reductions in size [6]. However, increasing nutrient supply, for example, might have the opposite effect, causing a body-size increase in some taxa [4,5].

Moreover, individual responses to warming might be even population-specific due to individual environmental requirements (availability of nutrients and oxygen) and metabolic specifications [8]. Individual living cephalopod taxa, such as squid (analogous to the fossil belemnites), as stenothermal organisms, respond rapidly to warming events, hatching at smaller size, undergoing fast growth rates over shorter lifespans and maturing younger at smaller size [9–11].

Reductions in body-size—coined the Lilliput effect [12]—have been widely reported from mass extinctions and evolutionary crises associated with environmental perturbations [13,14] including the Early Toarcian crisis [15]. However, their mechanisms and environmental drivers are still poorly understood [14], especially because the effects of environmental perturbations on an organism's body-size might depend on the biological scale of organization considered [2]. For instance, over longer evolutionary time scales, i.e. considering fossil assemblages, several mechanisms might contribute to the Lilliput effect, including increased mortality of juveniles, extinction or temporary disappearance of large taxa, preferential survival or origination of small-sized taxa or the temporary reduction in adult body-size of the surviving taxa [13,14]. All of these mechanisms could explain the Lilliput effect *sensu lato*. However, only the latter, i.e. a within-lineage body-size decrease, is considered to be the mechanism behind the Lilliput effect *sensu stricto*, which depicts a reduction in body-sizes within individual species through time [12]. Interestingly, extinction risk in marine molluscs during multiple mass extinctions has been associated with preferential extinction of smaller rather than larger species including the end-Permian and end-Cretaceous mass extinctions [7].

The Early Toarcian crisis is a multi-phased event characterized by environmental and biodiversity perturbations. One of these pulses corresponds to the Pliensbachian–Toarcian (Pli–Toa) boundary event and the second pulse corresponds to the Toarcian Oceanic Anoxic Event (T-OAE) [16,17]. The Pli–Toa boundary event (approx. 183.7 Ma, [18]) follows the cooling and regressive event of the Late Pliensbachian (Emaciatum = Spinatum Zone) in the northern Tethys and Iberia [19]. It corresponds to an increase in seawater temperature (up to 6°C, figure 1), concomitant with the beginning of a marine transgression [21,24–27] as well as a small negative carbon isotopic excursion [22,28]. The Pli–Toa boundary event records a crisis among planktonic [29,30], benthic [31] and nektonic organisms [32], expressed by extinction and changes in abundance and diversity. Despite marked extinction in ammonites [32], the few data existing on Pliensbachian European belemnite fauna do not allow recognition of the Pli–Toa boundary event as an extinction horizon, at least in northwest European basins [33–36].

After the Pli–Toa boundary event, the Polymorphum (=Tenuicostatum) Zone corresponds to a cooling phase [19,21,37] in the northern Tethys and Iberia, although it is comparatively warmer than the Late Pliensbachian. This cooling phase is followed by the T-OAE, starting at the base of the Levisoni Zone [18] and characterized by a marked increase in the seawater temperature (up to 7.5°C, figure 1), widespread anoxia and deposition of organic-rich sediments [17,21,22,38–40]. These important changes in the ocean–atmosphere system had a major impact on marine biota, causing body-size changes and extinction of particularly pelagic predators, such as ammonite species [15,32,41] and benthic suspension-feeding fauna [16,42–46]. The T-OAE also marks a major bottleneck in belemnite diversity and abundance [47] and might have triggered belemnite provincialism among Boreal–Arctic and northwest European faunas [48–50]. The increased anoxia during the T-OAE has been interpreted to contribute to the demise of many belemnite taxa, while *Acrocoelites* might have survived and radiated in its immediate aftermath [51]. The T-OAE coincides with an abrupt negative carbon isotopic excursion (CIE) which disrupts an overarching positive excursion [38,52–54], interpreted to reflect the enhanced burial of organic carbon and its preservation at the sea bottom. Although deoxygenation has been interpreted to increase since the Pli–Toa boundary, the negative CIE and widespread black shale deposition are still interpreted to reflect the peak of anoxia during the T-OAE [55].
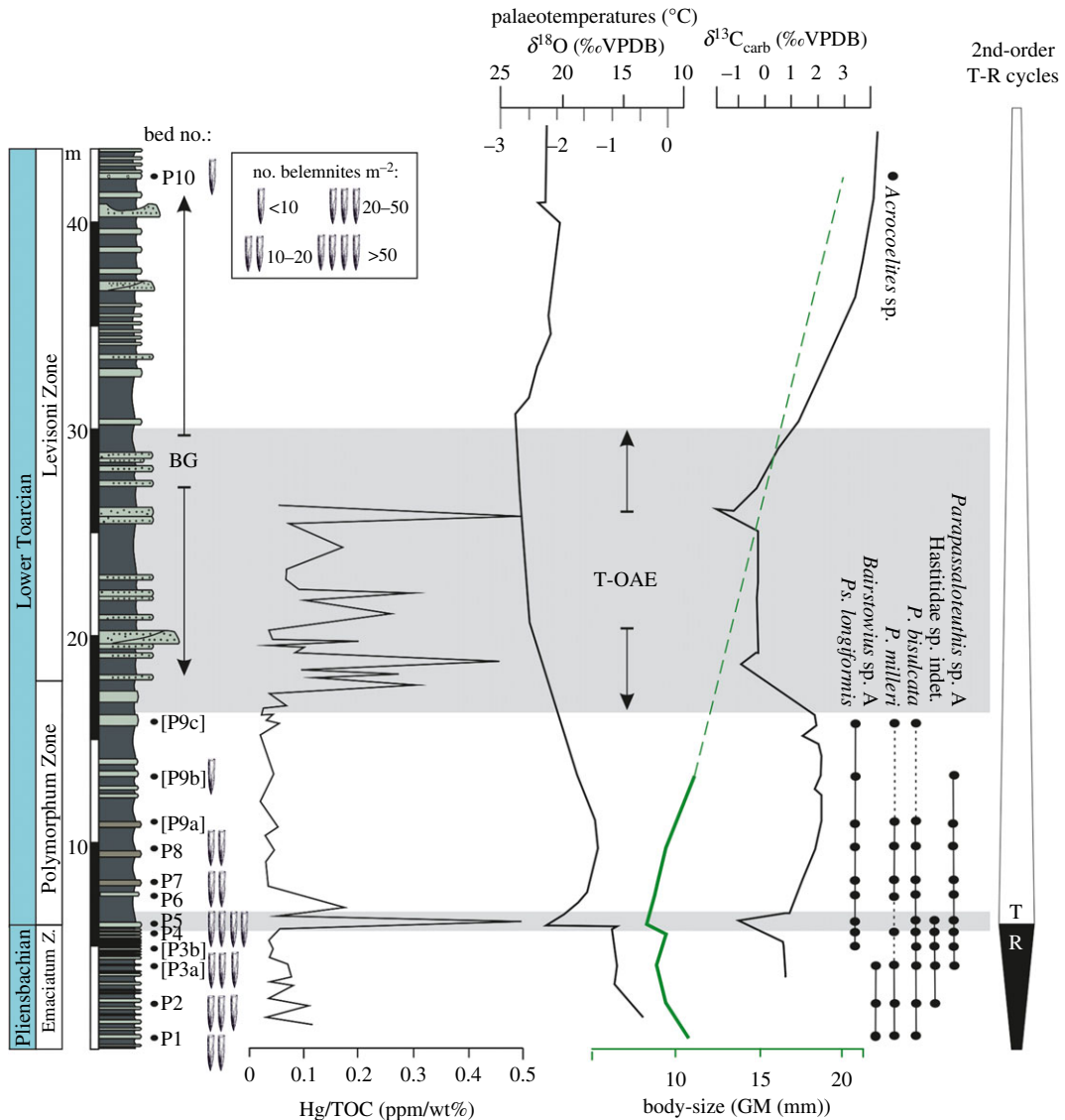
Figure 1. Variation of belemnite body-size (GM, assemblage scale), absolute abundance (no. belemnites m^{-2}) and stratigraphic ranges of species, compared with the variation of the analysed geologic proxies (mercury concentration, Hg/TOC [20], carbon and oxygen isotopes, $\delta^{13}C_{carb}$ and $\delta^{18}O$ [21,22]) and sequence stratigraphy data [23] from the Upper Pliensbachian–Lower Toarcian of Peniche. The shaded area highlights the Pli–Toa boundary event. The bed numbers in square brackets correspond to the beds that were merged due to sample size constraints, regarding the belemnite body-size analysis. See electronic supplementary material (figure S2) for details on belemnite abundance. See figure 5 for more information on lithology. Ammonite Zones: Emaciatum Zone, *Emaciaticeras emaciatum*; Polymorphum Zone, *Dactylioceras polymorphum*; Levisoni Zone, *Hildaites levisoni*. BG, belemnite gap; GM, geometric mean; T, transgressive; R, regressive.

Both warming events and the associated carbon cycle perturbations are considered a consequence of volcanic outgassing, either directly, by increasing pCO_2 in the seawater [56], or indirectly (i.e. by triggering other sources of isotopically light carbon [19]). In distal sections, enhanced mercury deposition is interpreted to be a proxy for constraining Karoo–Ferrar volcanism [20]. Irrespective of the controversy over the use of mercury as a proxy for volcanic outgassing [55], it is hitherto the best available proxy to temporally constrain the direct consequences of the rapid rise of pCO_2 in the seawater, including warming, deoxygenation and acidification.

In Peniche, mercury anomalies coincide with extreme climatic changes [20], expected to result in a body-size decrease [6,8]. By contrast, extreme climatic changes can increase weathering and precipitation, causing body-size increase instead, due to the input of nutrients [4,6]. However, despite the evidence for the increased weathering and influx of nutrients in Peniche [27], no indication of marked freshwater input or productivity increase [29] has been observed and, therefore, a reduction in body-size is expected. It is, however, worth noting that modern systems have shown us that the interaction between climate change,

nutrient input and productivity is complex and might vary regionally (e.g. [57]) and according to the scale considered [58]. Additionally, such variations might be difficult to constrain in the geological record without modelling—so far only available for a limited number of time-slices, such as at the Palaeocene–Eocene Thermal Maximum [59,60].

Belemnites are coleoids closely related to extant teuthids (such as squid). They are very abundant and diverse in the fossil record and played an important role in Jurassic ecosystems (e.g. [61]). Most of the research on Lower Jurassic belemnites was focused on the geochemistry of northwest European basins [51,62–64], temperate zones where the regional extent of anoxia was great [48,61]. The only study on belemnite body-size has been focused solely on two genera and found an ambiguous response to crisis events [15]. Therefore, a high-resolution analysis of belemnite body-size during the past episodes of environmental crisis will provide valuable insights on the response of cephalopods to the global change observed in modern marine ecosystems.

The Peniche reference section is well studied in terms of geochemistry and stratigraphy [20,22,23,27,65] and yields a highly abundant belemnite fauna, allowing for the first time the analysis of (i) the mechanisms behind belemnite body-size fluctuations, at different scales of organization (individual ontogenetic, species and assemblage), during the Pliensbachian–Toarcian interval, in subtropical latitudes and (ii) their potential environmental drivers—mainly temperature, carbon cycle and changes in pCO_2 associated with volcanism. We hypothesize, on the one hand, a within-lineage reduction (Lilliput effect *sensu stricto*) in belemnite body-size across the Pli–Toa boundary event and, on the other hand, a body-size increase across the T-OAE, driven by species turnover in the Peniche section.

# 2. Material and methods

2.1. Taxonomy and ontogeny

Belemnite species identification was based on the analysis of traditional features, such as shape (outline and profile) and the presence of grooves in the apical region (e.g. [35]). The transverse section, the depth of penetration of the alveolus, and the apical line were all observed using CT scanning. These features were afterwards compared with the published descriptions and figures. This method also allowed us to recognize the features of each ontogenetic stage with the acquired longitudinal sections, making it possible to distinguish between adult (Neanic–Ephebic–Gerontic *sensu* [61]) and juvenile (Nepionic *sensu* [61]) specimens (electronic supplementary material, figures S1 and S2), especially by having the possibility of observing the growth increments of the rostra. The taxonomic composition of the belemnite assemblages across the studied interval is in conformity with the data from contemporaneous Tethyan sections [35,36,47,50,61,66,67]. Seven taxa compose the belemnite assemblages in the Peniche section (figure 1; electronic supplementary material, figures S1 and S2).

2.2. Sampling methods and belemnite body-size proxies

The specimens were collected from 13 beds (stratigraphic horizons) sampled from 45 m of the Upper Pliensbachian–Lower Toarcian sediments, corresponding to the Upper Emaciatum–Upper Levisoni ammonite zones (figure 1, approx. 2.7 Ma, [18]). As belemnites become rarer up section, the data derived from beds P9a, P9b and P9c were pooled to obtain a reasonable sample size for a quantitative analysis (figure 1). The same conservative approach was adopted for beds P3a and P3b.

We focused on quantitatively collecting from well-exposed bedding planes of limestones, marly limestones and marls. A total of 930 belemnite rostra were collected by (i) sampling all specimens within 14 one-square-meter areas and (ii) by collecting at least 30 complete specimens in the remaining bed area, i.e. outside of the quadrats. This first sampling method allowed the calculation of absolute abundance, taking into account both fragmented and complete specimens. The body-size analysis was based only on the complete specimens, regardless of the sampling method. The more complete belemnites are suspected to be a less time-averaged sample [68], because a better preservation is usually an indicator of quick burial and little transport of the fossil. Conveniently, complete specimens (with at least part of the alveolar region preserved) are easier to assign taxonomically and ontogenetically [69]. The fragmented specimens were only used to calculate the belemnite abundance per bed.

The rostrum represents a considerable part of the belemnite animal, and it is hypothesized that it acts as a counterbalance for the soft tissue and phragmocone [70], despite the increasing number of studies suggesting an original partially porous rostrum structure [71,72]. However, in all known belemnites
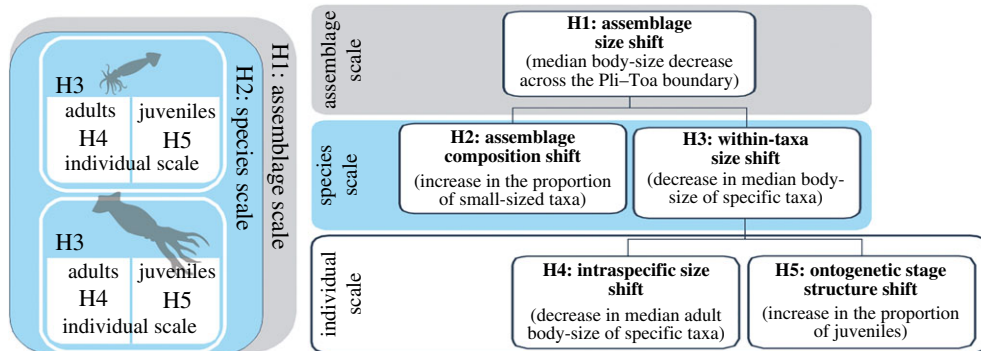
Figure 2. Conceptual scheme depicting the tested hypotheses regarding the mechanisms behind belemnite body-size reduction, at different palaeobiological scales of organization.

with soft tissue preservation, the fins attach to the rostrum and the soft parts closely track the outline of their internal skeleton, as in their extant relatives [73,74]. For these reasons, the rostrum can be considered a reasonable proxy for body-size in the absence of the preserved soft tissue [69]. This is also supported by a comparison between hard parts and soft parts in well-known taxa showing that larger rostra correspond to a larger mantles [75]. It is noteworthy that most of the studied specimens did not bear epirostra and, therefore, only the orthorostra were considered for the morphometric analysis. As for the epirostrum-bearing specimens, only the orthorostrum was measured.

Previous research has demonstrated that the geometric mean (GM), a unidimensional metric that combines the apical height, width and length $\left(\mathrm{GM} = \sqrt[3]{\mathrm{Dv} \times \mathrm{Dl} \times l} \right)$ is the most robust proxy to compare the body-size between morphologically different forms belonging to different species or ontogenetic stages within a species [69]. In addition, the geometric mean is more comparable to the proxies used in extant coleoids [76]. In order to calculate the GM, 277 of the complete specimens were CT scanned to allow the calculation of this metric in a non-destructive way, since the alveolus was filled with sediment, precluding direct measurement (see electronic supplementary material, table S7 for details on the settings). Additionally, 109 specimens were measured with a calliper, since the alveolus was empty. The relative change in volume better reflects changes in absolute body-size proxies used in extant taxa (e.g. weight). We, therefore, a proxy for the rostrum volume (GM^3) to express relative volumetric changes.

2.3. Mechanisms of body-size changes

The mechanisms behind the belemnite body-size fluctuations through time, from the assemblage to the individual scale of organization, were assessed by testing a set of hierarchical hypotheses (H), modified from [2] (figure 2). The first hypothesis predicts a decrease in the mean body-size at the assemblage scale, regardless of the underlying mechanisms (assemblage size shift hypothesis, H1, figure 2). If H1 is validated, there are four subsequent hypotheses that could explain this decrease [2,8]. First, an increase in the proportion of small-sized species (assemblage composition shift hypothesis, H2). Second, a decrease in the median body-size within specific taxa (within-taxa size shift hypothesis, H3), which could, in turn, be related to a decrease in adult body-size (intraspecific size shift hypothesis, H4). The last hypothesis associates the decrease in the mean body-size with an increase in the proportion of juveniles (ontogenetic stage structure shift hypothesis, H5).

The whole set of hypotheses could explain the Lilliput effect *sensu lato*, although only H4 relates to the Lilliput effect *sensu stricto*, as predicted by the temperature-size rule in extant coleoids [77]. Note that, in comparison with recent data, the interpretation of body-size changes based on fossil data is more complex because fossil assemblages reflect not only a past biotic community, but also the mortality and preservation of the organisms that were part of it.

At the assemblage scale of organization, H1 was tested by assessing the size distribution of the whole assemblage through time. The proportional change in body-size was calculated between stratigraphically consecutive beds (example: bed_t and bed_{t+1}) in percentage of the log ratio (example: $\ln(\mathrm{median\ bed}_{t+1}/\mathrm{median\ bed}_t) \times 100\%$). The median belemnite body-size (geometric mean) was calculated for each bed. The whole distribution and the median were compared using the non-parametric Mann–Whitney U and Kolmogorov–Smirnov tests to assess the significance

of the belemnite body-size differences between consecutive beds (electronic supplementary material, table S2). This was done at the assemblage and species scales (electronic supplementary material, table S2).

Because changes in taxonomic composition can influence the body-size patterns by the appearance and/or disappearance of taxa, we modified the within- and among-taxa approach by Rego *et al*. [78]. This method corresponds to a pair-to-pair analysis (comparison of stratigraphically successive beds, t and $t + 1$), focused on the taxa identified in stratigraphically successive beds (boundary crossers). This method allows division of the assemblage body-size shift (equation (2.1)) into three components: a disappearance of taxa effect (equation (2.2)), a within-lineage effect (equation (2.3)) and an appearance of new taxa effect (equation (2.4)).

$$\text{assemblage size shift} = \text{assemblage median body-size}_{\text{bed}\,t+1} - \text{assemblage median body-size}_{\text{bed}\,t}, \quad (2.1)$$
$$\text{disappearance of taxa effect} = \text{boundary crossers}_{\text{bed}\,t} - \text{all taxa}_{\text{bed}\,t}, \quad (2.2)$$
$$\text{within-lineage effect} = \text{boundary crossers}_{\text{bed}\,t+1} - \text{boundary crossers}_{\text{bed}\,t} \quad \text{and} \quad (2.3)$$
$$\text{appearance of new taxa effect} = \text{all taxa}_{\text{bed}\,t+1} - \text{boundary crossers}_{\text{bed}\,t+1}. \quad (2.4)$$

Finally, at the individual ontogenetic scale of organization, the hypotheses were tested by assessing the body-size variation within different ontogenetic stages (adults and juveniles) for individual taxa. Variation partitioning allowed us to assess the proportion of body-size (geometric mean) variation explained by ontogeny, taxonomic assignment and separation by beds and by their joint effects. If the fraction of variation corresponding to beds separation is low, this suggests that mechanisms driving differences between samples are similar and not related to particularities of the sample (e.g. lithology and age). Variation in the body-size data was partitioned using partial redundancy analysis (RDA), as implemented in the *vegan* package in R [79,80]. The significance of each fraction was assessed through the analysis of variance (ANOVA). The whole time-series was compared with the Pli–Toa boundary event.

## 2.4. Environmental drivers of body-size changes

In order to test our hypothesis of a relationship between belemnite body-size and environmental perturbations, the distribution of the GM was compared with three main geologic proxies (table 1). These are brachiopod stable oxygen isotopes [21], bulk rock carbon isotopes [22] and bulk rock mercury concentration normalized by total organic carbon [20], used as proxies for seawater palaeotemperature, negative excursions in the carbon cycle and volcanogenic outgassing, respectively (table 1). To account for the impact of sedimentary properties on body-size patterns, we corrected for the effect of lithology and belemnite absolute abundance (mean abundance of belemnites m^{-2}, figure 1; electronic supplementary material, figure S3) by residualizing [84]. A simple linear regression analysis is performed between the body-size and the combined effect of abundance and lithology. The residuals from this analysis are then used as outcome in the ultimate regression analysis between body-size and abiotic variables. All variables of the model were continuous with the exception of lithology. We assigned our samples a categorical variable for lithology (marl to limestone) based on carbonate/clay content. Collinearity between explanatory variables was tested by using *cor* function in R (electronic supplementary material, figure S5). Sedimentary properties and various other parameters linked with climate warming (such as strontium isotopes, total organic carbon and abundance of primary producers) could not be directly included in the models due to their high collinearity with $\delta^{13}C_{\text{carb}}$ or the other two parameters used (electronic supplementary material, figure S4); hence, the choice of the abiotic parameters is indicated in table 1.

A multiple linear regression using generalized least squares (GLS) was performed and the models were fitted by maximizing the log-likelihood (*gls* function in R). The first-order autoregressive (AR(1)) model was used, which has the property of seeking autocorrelation and of minimizing the error term in a time-series [85]. Seven models (see electronic supplementary material, R script) were compared using Akaike's second-order corrected information criterion (AICc scores), which corrects for small sample size. The power of the best model was assessed by means of an ANOVA test. The statistical significance of each coefficient of the best model was assessed by calculating the *p*-value under a *t* approximation. The significance level was $p < 0.05$ for all the analyses, unless stated otherwise. The analyses were performed in R [80], using the packages *nlme* [86] and *qpcR* [87].

The regression analysis only included data from Emaciatum and Polymorphum zones (beds P1–P9), due to the lack of a representative sample size in the Upper Levisoni Zone (bed P10, figure 1).

Table 1. Environmental constraints (abiotic parameters) based on their geological proxies and their theoretical role in mediating body-size changes and their interpretation in the context of the Lusitanian Basin.

geologic proxy [source]	environmental variable	basis	interpretation in the context of the LB	theoretical controls on body-size
brachiopod stable oxygen isotope ratio (δ^{18}O) [21]	dominantly bottom seawater temperature	Temperature-dependent isotopic fractionation between carbonate minerals and seawater [81]	High temperatures during negative excursions	Increasing temperature through various mechanisms including the increase of both growth and development rates are expected to lead to a smaller adult body-size [8].
δ^{13}C $_{carb}$ [22]	carbon cycle perturbations related to anoxia	Isotopic fractionation between photosynthesizers and seawater. Photosynthesizers remove light C^{12} from the seawater and this is incorporated into the sea bottom sediment after burial as organic carbon [82].	Negative excursions during the Early Toarcian reflect enhanced burial of organic carbon during the zenith of anoxia [83]. They could also be influenced by increased primary production but are interpreted to reflect rather widespread oxygen depletion as primary productivity is interpreted to have dropped during these intervals [29,30].	At the edge of an organism's temperature range, growth is usually impaired by insufficient energy or oxygen supply, decreasing both growth rate and body-size at any developmental stage [8].
Hg/TOC ratio [20]	volcanogenic outgassing	Volcanism represents a source of mercury to the atmosphere. Due to rain or run-off, mercury moves from the terrestrial realm/atmosphere to the marine realm in mineral form or adsorbed in detrital organics. Hg burial is limited by low abundance and/or burial of organic matter or sulfides that would scavenge aqueous Hg [20,55].	Hg anomalies (high Hg/TOC ratio) in the sediment are interpreted to represented markers of volcanism in distal sections. They have been interpreted to reflect volcanic outgassing, but their interpretation in some distal sections might be more complex [55].	Increasing pCO_2, combined with increasing temperature, causes a decrease in both dissolved oxygen and pH of the seawater. In association with other factors related to rapid warming, such as weathering and eutrophication, these factors are expected to lead to a body-size decrease due to their direct effects on the availability of food resources [6].
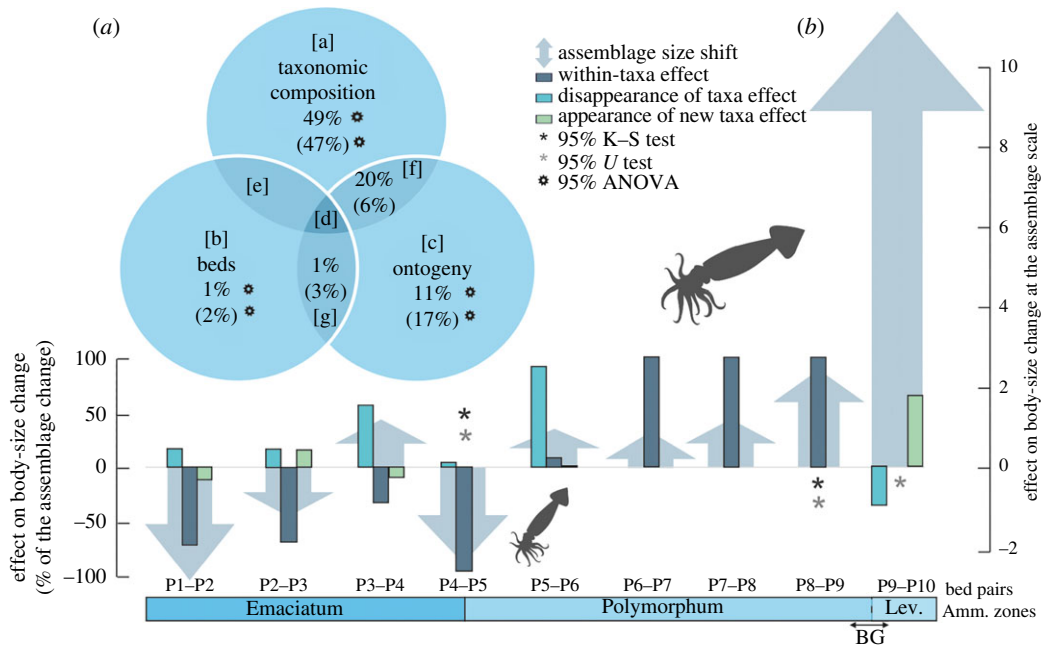
Figure 3. (a) Venn diagram depicting the partition of belemnites body-size variation between taxonomic composition, bed separation and ontogeny. The values between parentheses correspond to the whole time-series and the values without parentheses correspond to the Pli–Toa boundary. See the 'Material and methods' section for more details on the variation partitioning methodology. (b) Effect on body-size change at the assemblage and species scale of organization. The bed pairs in the horizontal axis represent pairwise comparisons. See electronic supplementary material (table S6) for details. For a correct interpretation of the right-side scale, the bottom of the arrowhead should be considered, rather than the tip of the arrow. Note that the x-axis depicts comparisons of consecutive pairs of beds (not to scale). BG, belemnite gap; U-test, Mann–Whitney U-test; K–S test, Kolmogorov–Smirnov test.

3. Results

3.1. Belemnite body-size fluctuations

3.1.1. Assemblage scale

A total of seven belemnite species were identified in Peniche (figure 1). Most of the taxa range from the uppermost Pliensbachian to the Lower Toarcian (uppermost Polymorphum Zone). *Bairstowius* sp. A is exclusively represented in the uppermost Pliensbachian, being stratigraphically replaced by *Pseudohastites longiformis* in the assemblage. In the Toarcian, the Levisoni Zone is devoid of belemnites, with the exception of bed P10 (Upper Levisoni Zone) which includes two specimens assigned to *Acrocoelites* sp. (figure 1).

Three episodes of the median rostrum size decrease were recognized at the assemblage scale across the studied interval: between beds P1 and P2, between bed P2 and P3 and at the Pli–Toa boundary event (beds P4 and P5). Only the latter corresponds to a statistically significant decrease (p-value Kolmogorov–Smirnov test = 0.01; p-value Mann–Whitney U-test = 0.04; figure 3b) and corresponds to a 13% body-size decrease (figure 4). This decrease in the belemnite body-size proxy (GM) corresponds to a 40% decrease in rostrum volume (electronic supplementary material, table S2).

The assemblage body-size shift at the Pli–Toa boundary event is almost exclusively caused by the boundary crossers *Ps. longiformis*, *P. bisulcata* and Hastitidae sp. indet. (within-taxa effect; figure 3b). The taxonomic composition across the boundary does not change markedly, with *Ps. Longiformis*, the most abundant taxon, comprising 61.9% (bed P4) and 56.2% (bed P5) of the assemblages (figures 1 and 4). The disappearance of *Passaloteuthis milleri* and *Parapassaloteuthis* sp. at the Pli–Toa boundary event causes 4% of the decrease in the assemblage median body-size (disappearance of taxa effect; figure 3b).

By contrast, the other two episodes of body-size reduction (between beds P1 and P2 and between beds P2 and P3) are mainly related to the appearance (15.9 and 16.2%, respectively) and disappearance of taxa (12.1 and 15.2%, respectively), but also to the body-size decrease in specific taxa (within-taxa effect; (figure 3b). The within-taxa effect on the assemblage body-size shift between beds P1 and P2 and between beds P2 and P3 (72%; 69%) is, however, lower than at the Pli–Toa boundary (96%, figure 3).
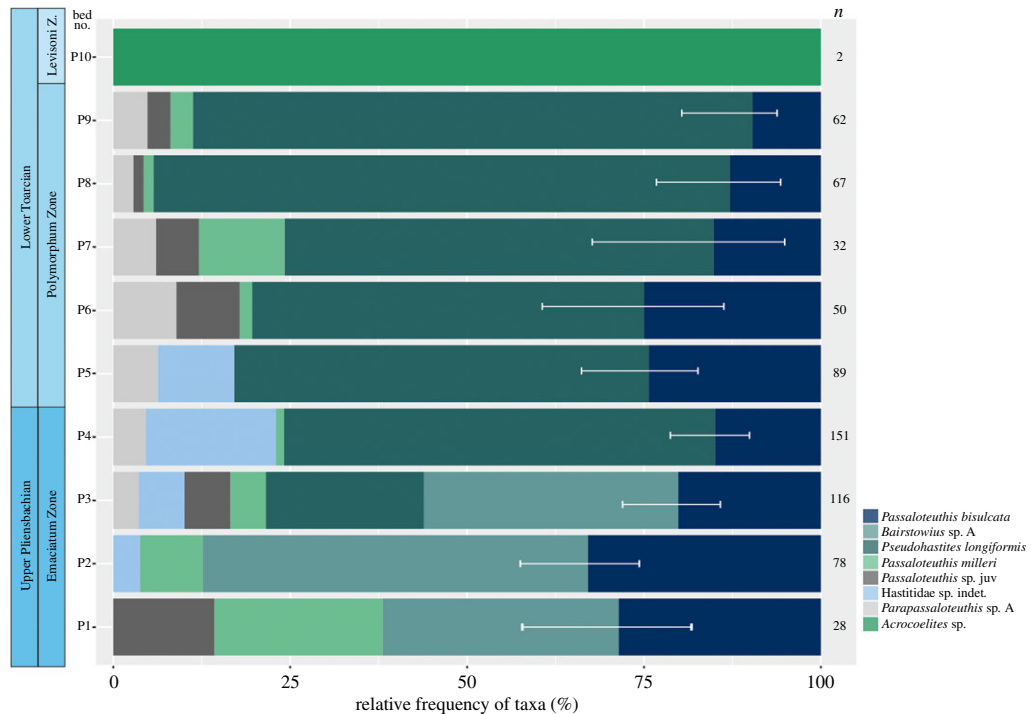
Figure 4. Relative frequency of the different taxa comprising the Upper Pliensbachian–Lower Toarcian Peniche belemnite assemblage. Note that determinable incomplete specimens were also taken into account and so sample size (*n*) differs between figures 4 and 5. The error bars correspond to the 95% confidence interval of the relative frequency of the species *Ps. longiformis/Bairstowius* sp. A and *P. bisulcata*, the most abundant taxa.

At the assemblage scale, an increase in the median body-size is observed between beds P3 and P4, P5 and P6, P7 and P8, P8 and P9 and between P9 and P10. However, only the bed pairs P8–P9 and beds P9–P10 correspond to significantly different body-sizes (figure 3*b*).

In sum, across the studied interval at the assemblage scale, a significant decrease in belemnite body-size is observed across the Pli–Toa boundary (beds P4 and P5). After that, from bed P5 to bed P9, a general increase in belemnite body-size is observed, followed by a belemnite gap, from bed P9 to bed P10 (figures 3*b* and 5), during which no belemnites occur.

3.1.2. Species scale

Three taxa (*Ps. longiformis*, *P. bisulcata* and Hastitidae sp. indet.) are recorded immediately before and immediately after the Pli–Toa boundary event (boundary crossers; figure 1). The most significant and largest reduction in size is observed in *Ps. longiformis*, the most abundant taxon (17% decrease in GM and 51% in rostrum volume; figure 6).

Despite the lack of statistical significance, *P. bisulcata*, the second most abundant taxon, also decreases in size (7% in GM and 21% in volume, figure 6) across the Pli–Toa boundary event, while Hastitidae sp. indet., slightly increases in size (8%, electronic supplementary material, figure S7). It is noteworthy that *P. bisulcata* body-size markedly decreases (109%, figure 6) immediately after the Pli–Toa boundary event, from bed P5 to bed P6 (lowermost Polymorphum Zone), which is coincident with the extirpation of Hastitidae sp. indet. (figure 1).

3.1.3. Individual ontogenetic scale

Considering the whole time-series, the variation partitioning analysis results revealed that taxonomic composition (47%) and ontogeny (17%) are responsible for most of the variation in belemnite body-size. The separation by bed explains only 2% of the body-size variation (figure 3*a*, values between parentheses).

At the Pli–Toa boundary event, the body-size variation partitioning into taxonomy and ontogeny is similar to what is observed for the whole time-series (49 and 11%, respectively). However, the joint effect of taxonomy and ontogeny explains 20% of the variation in body-size, in contrast with the 6% observed for the whole time-series (figure 3*a*, values without parentheses). This probably suggests that across the Pli–Toa boundary event, ontogenetic stages behave more similarly among taxa in explaining body-size variation.
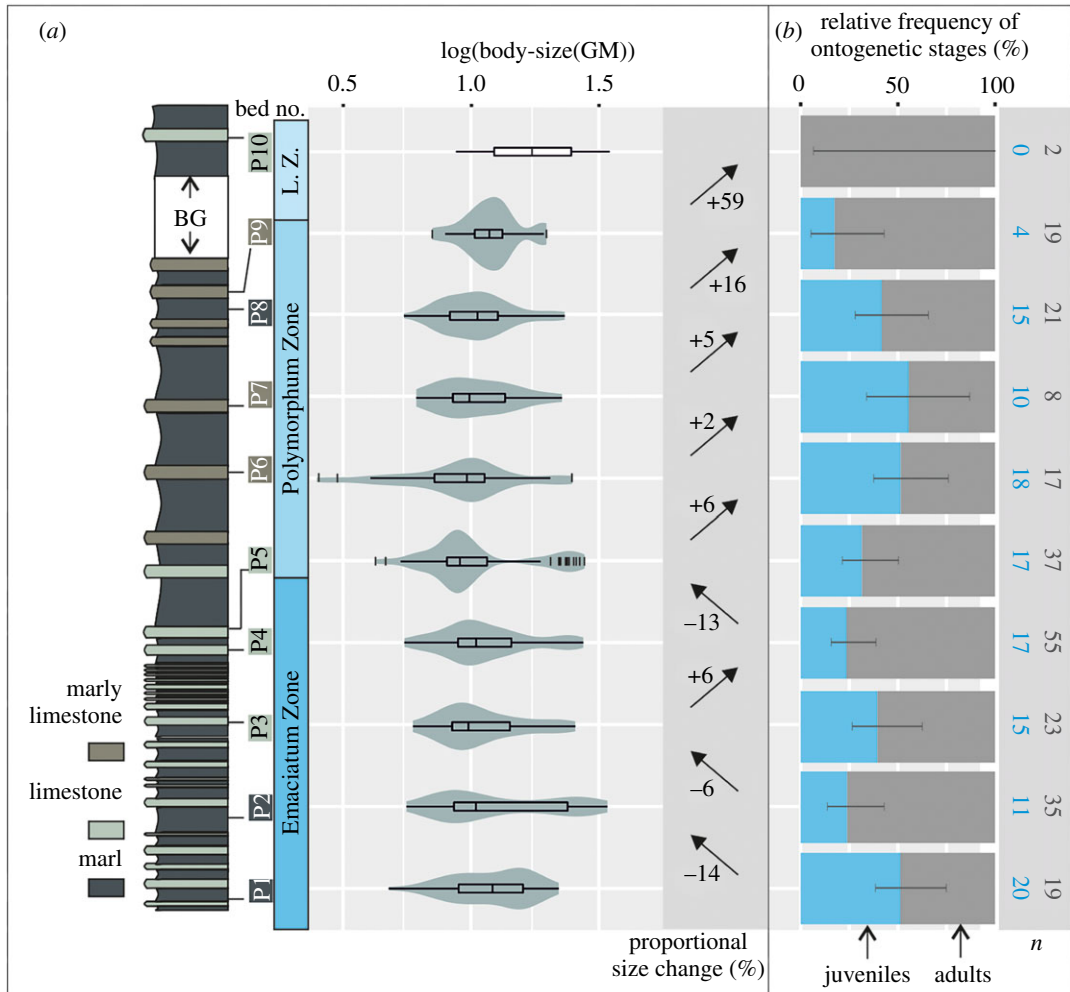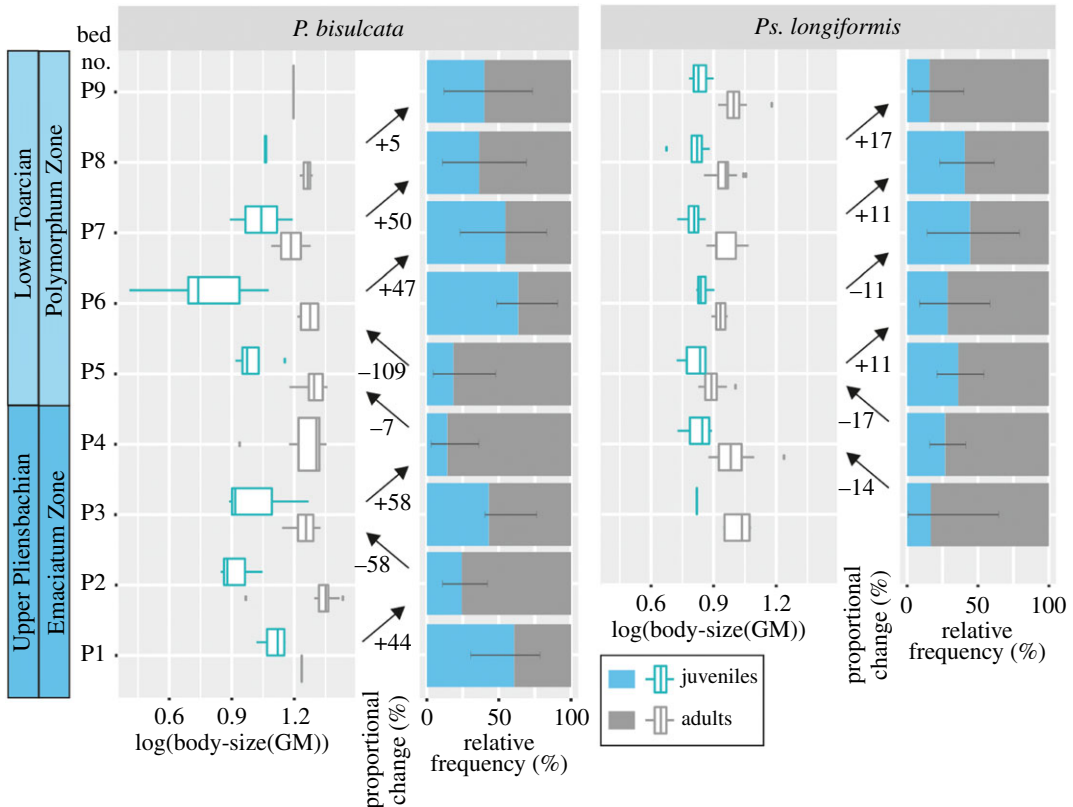
Figure 5. (*a*) Lithology, belemnite body-size variation (violin plots) and proportional body-size change across the studied interval in Peniche. (*b*) Relative frequency of ontogenetic stages at the assemblage scale across the studied interval in Peniche. Note that the stratigraphic log is not drawn to scale, for real thickness of beds, see figure 1. The error bars correspond to the 95% confidence interval of the juveniles and adults ratio. BG, belemnite gap; GM, geometric mean; *n*, sample size.

At the individual ontogenetic scale of organization, only the adult specimens of *Ps. longiformis* recorded a significant (Kolmogorov–Smirnov test p-value $= 2.61 \times 10^{-6}$; Mann–Whitney U-test p-value $= 3.98 \times 10^{-7}$) body-size decrease across the Pli–Toa boundary event (21%, electronic supplementary material, table S2). The ratio adult versus juveniles of *Ps. longiformis* does not change significantly across the Pli–Toa boundary event (31.25%, figure 6).

A reduction of 7% (although not significant) in adult body-size is observed in *P. bisulcata* specimens, across the Pli–Toa boundary event, together with a slightly increased percentage of juveniles of the same species (figure 6). Immediately after the boundary, from bed P5 to bed P6, a marked reduction (109%) in *P. bisulcata* body-size is recognized mainly among the juvenile specimens, in tandem with a decrease in their proportion (from 75 to 68.75%, figure 6).

3.2. Relationship with environmental parameters

After correcting for the effects of sedimentary properties (lithology and fossil abundance), the results of the regression analysis revealed that the variation in belemnite body-size is best correlated with the variation in δ^{18}O (table 2, model no. 5), at the assemblage scale. The overall model is significant (electronic supplementary material, table S3), suggesting a body-size reduction with increasing δ^{18}O values/decreasing seawater temperature values (electronic supplementary material, figure S2). However, the models combining δ^{18}O with δ^{13}C$_{carb}$ (model no. 2, table 2) and combining Hg/TOC with δ^{13}C$_{carb}$ (model no. 3, table 2) could not be rejected, according to the AICc scores ($\Delta < 2$). If the

Figure 6. Belemnite body-size variation (GM), proportional body-size change and relative frequency of ontogenetic stages across the Upper Pliensbachian–Lower Toarcian of Peniche at species scale (P. bisulcata and Ps. longiformis). Passaloteuthis genus was used to calculate the relative frequency of ontogenetic stages of P. bisulcata due to the difficulty of a species-level classification of the juvenile specimens of Passaloteuthis genus. The error bars correspond to the 95% confidence interval of the juveniles and adults ratio. For sample size, see electronic supplementary material (figure S6). GM, geometric mean.

data are not corrected for the effects of the sedimentary properties, the same results are obtained, despite minor differences in significance (electronic supplementary material, table S5).

After correcting for the effects of sedimentary properties, when considering the most abundant taxon, *Ps. longiformis*, the best model explaining the body-size variation includes solely Hg/TOC (model no. 6, table 2). However, the effects of $\delta^{18}O$, $\delta^{13}C_{carb}$ and Hg/TOC cannot be discarded, since, statistically, the model nos. 5, 2 and 4 cannot be distinguished from model no. 6, according to the AICc scores. If the data are not corrected for the effects of lithology and abundance beforehand, model no. 4 (Hg/TOC + $\delta^{18}O$) best explains *Ps. longiformis* body-size variation, with highly significant results (electronic supplementary material, table S5). The role of Hg/TOC in the model is more significant than the role of $\delta^{18}O$ (electronic supplementary material, table S4b).

After correcting for the effects of lithology and fossil abundance, *P. bisulcata* body-size is best correlated with Hg/TOC (model no. 6, table 2), as well, despite the lack of significance (table 3). However, the effects of $\delta^{18}O$, $\delta^{13}C_{carb}$ and Hg/TOC cannot be disregarded, since statistically model nos. 5, 2 and 4 cannot be distinguished from model no. 6. If no correction is applied beforehand, the model no. 4 (Hg/TOC + $\delta^{18}O$) best explains the *P. bisulcata* body-size variation, with highly significant results (electronic supplementary material, table S5).

4. Discussion

4.1. Scales and mechanisms of body-size variation

4.1.1. Pli–Toa boundary event

Body-size reductions have been identified in several episodes of biotic/abiotic crisis, many times related to warming. Body-size fluctuations in fossil assemblages are common and can be caused by a variety of

Table 2. AICc ranking of models describing the effect of palaeotemperature (δ^{18}O), carbon cycle perturbations (δ^{13}C$_{carb}$) and volcanism (Hg/TOC) on belemnites body-size (GM) for the assemblage and species scale (*Ps. longiformis* and *P. bisulcata*), corrected for the effects of sedimentary properties (lithology and belemnite abundance). Only the models with $\Delta < 2$ are listed. See electronic supplementary material (table S4) for the full list of GLS models.

	model no.	Δ	AICc scores	ANOVA *p*-value
assemblage				
GM $\sim$ 1	null	5.09	1921.87	—
GM $\sim \delta^{18}$O	**5**	0	1920.92	0.0849
GM $\sim \delta^{18}$O $+ \delta^{13}$C$_{carb}$	2	1.99	1922.91	
GM $\sim$ Hg/TOC $+ \delta^{13}$C$_{carb}$	3	1.91	1922.84	
Ps. longiformis				
GM $\sim$ 1	null	2.51	671.37	—
GM $\sim$ Hg/TOC	6	0	668.87	0.0327
GM $\sim \delta^{18}$O $+ \delta^{13}$C$_{carb}$	2	0.87	669.74	
GM $\sim$ Hg/TOC $+ \delta^{18}$O	4	1.31	670.17	
GM $\sim \delta^{18}$O	5	0.50	669.37	
P. bisulcata				
GM $\sim$ 1	null	−1.46	607.97	—
GM $\sim$ Hg/TOC	6	0	609.43	0.4306
GM $\sim \delta^{13}$C$_{carb}$ $+$ Hg/TOC	3	1.87	611.30	
GM $\sim \delta^{18}$O	5	0.35	609.78	
GM $\sim \delta^{13}$C$_{carb}$	7	0.58	610.01	

Table 3. Details of the selected GLS models comparing belemnite body-size (GM) with palaeotemperature (δ^{18}O), carbon cycle perturbations (δ^{13}C$_{carb}$) and volcanism (Hg/TOC), corrected for the effects of sedimentary properties (lithology and belemnite abundance). GM, geometric mean; s.e., standard error; d.f., degrees of freedom.

scale	model no.	coefficients	value	s.e.	*t*-value	*p*-value	d.f.	residual
assemblage	5	intercept	2.44	1.48	1.64	0.1019	340	338
		δ^{18}O	2.04	1.19	1.72	0.061	—	
Ps. longiformis	15	intercept	0.31	0.23	1.32	0.1904	160	158
		Hg/TOC	−2	0.93	−2.14	0.0335	—	
P. bisulcata	5	intercept	0.43	0.94	0.46	0.6458	101	99
		Hg/TOC	−3.15	4.02	−0.78	0.4358	—	

mechanisms. Our goal is to test the effect of warming and related stressors in belemnite body-size dynamics across the Pliensbachian–Toarcian crisis recoded in the Peniche section.

Statistical evaluation of our data has shown that size changes of belemnite rostra in the studied section at Peniche are significant for the Pliensbachian–Toarcian boundary event, i.e. the assemblage size shift hypothesis (H1) was validated. This size change is almost exclusively driven by a body-size reduction of single species—*Ps. longiformis*, allowing us to validate the within-taxa size shift hypothesis (H3). No marked changes in the proportion of ontogenetic stages of *Ps. longiformis* are observed at the Pli–Toa boundary event, meaning that the largest within-lineage body-size change is not due to changes in the ontogenetic structure of the population, but rather to an adult body-size reduction. In conclusion, at the individual ontogenetic scale, we were able to validate the intraspecific size-shift hypothesis (H5), across the Pli–Toa boundary event, finding a 51% decrease in rostrum volume (21% in median GM) of adult specimens of *Ps. longiformis*. By contrast, *P. bisulcata* body-size reduction is a combination of increased percentage of juveniles (increased mortality of juveniles) and reduction in adult body-size.

The Lilliput effect *sensu lato* was already identified within particular cephalopod species in the Cleveland Basin, interpreted as a response to the deteriorating environmental conditions associated with the Early Toarcian crisis [15]. However, this work does not explicitly take into account ontogeny (e.g. impact of the changes in the proportion of ontogenetic stages on body-size). Similarly, among extant squid, maturation at small size and young age is interpreted as a life-history strategy to cope with warming events [9].

The differential taxa response found in our study might indicate different environmental tolerances, related to individual physiology or life-history strategies [8]. The only important morphological difference detectable from the fossilized remains between *Ps. longiformis* and the other taxa is the presence of an epirostrum, a calcified structure which develops in late ontogenetic stages [88] as an extension of the orthorostrum. It has been interpreted that the development of an epirostrum facilitates the animals' movement in the water by gliding as counterbalance to the development of specialized reproductive organs [88,89]. The increased pCO_2 that characterizes the environmental crisis of the Early Toarcian in Peniche [21] could directly (through calcification) or indirectly (through nutrient availability) have affected the calcification potential of the epirostrum. However, further data need to be assembled in order to assess the physiological and environmental constraints of the development of such a structure.

According to our results, a belemnite body-size reduction is observed at the Pli–Toa boundary event in Peniche. However, no major changes in the belemnite taxonomic composition are observed (figure 4), despite being considered one of the early pulses of the Early Toarcian crisis—particularly in ammonoid cephalopods [32]. This is consistent with the data available from other regions at higher latitudes [36,37,61,67], which demonstrate that the T-OAE, by contrast, corresponds to an important turnover in belemnite species [47]. In fact, the T-OAE had greater impact on marine biota than the Pli–Toa boundary event (e.g. [16,32,41,42], namely in the Lusitanian Basin, where planktonic and benthic organisms were largely affected [29,30,90–92]. This highlights the deterioration of the environmental conditions during the Early Toarcian, starting at the Pli–Toa boundary event and culminating in the T-OAE, an interval barren of belemnites in Peniche, as indicated by our results and previous studies [65].

4.1.2. The aftermath of Pli–Toa boundary event

Notwithstanding the decrease in seawater temperature during the early Polymorphum Zone, this interval is characterized by palaeoenvironmental perturbations, as evidenced by the carbon isotopic record [21,22]. Moreover, seawater temperature is still higher than during the Late Pliensbachian [21]. The conditions are, however, not as severe as during the Pli–Toa boundary event, or during the onset of the T-OAE, which is also supported by the response of other groups of marine biota in the Peniche section [29,30,90–92].

Passaloteuthis bisulcata body-size decreases during the aftermath of the Pli–Toa boundary event (109% from bed P5 to bed P6, early Polymorphum Zone) due to an increase in the relative proportion of juveniles of that species (figure 6). This might indicate the temporary emigration of large adults [9] and/or higher juvenile mortality due to the unsuitability of the habitat, as interpreted for fish and cephalopod species [93,94]. However, we also cannot rule out the existence of smaller (stunted) adults [9] which might not develop typical adult features [95], but this could only be disentangled with further studies, namely with a sclerochronological analysis.

The decrease in *P. bisulcata* body-size in the aftermath of the Pli–Toa boundary event coincides with an increase in adult body-size of *Ps. longiformis,* and with the disappearance of Hastitidae sp. indet. It is tempting to assume that the rapid recovery of *Ps. longiformis* potentially triggered a change in the belemnite population dynamics, potentially due to the competition for food resources, causing the emigration of some species (Hastitidae sp. indet.) and the increased mortality and stress in the early growth of others (*P. bisulcata*). A shift in distribution to cooler latitudes with warming is considered one of the most important responses in modern marine ecosystems [96,97].

Furthermore, the rest of the Polymorphum Zone (i.e. from bed P6 to bed P9) is characterized by an increase in *Ps. longiformis* body-size and abundance (and less relative mortality of juveniles), relatively to *P. bisulcata.* The latter becomes less abundant and maintains its adult body-size, emphasizing a potential competition between the *Ps. longiformis* and *P. bisulcata*. However, the fact that there is no increase in the proportion of *Ps. longiformis* comparatively to the proportion of *P. bisulcata*, from bed P5 to bed P6 (figure 6), is not entirely compatible with this interpretation and highlights the constraints of testing the effects of competition and other biotic parameters on body-size in fossil assemblages.

4.1.3. T-OAE

The interval corresponding to the onset of the T-OAE in Peniche is barren of belemnites, starting around the Polymorphum–Levisoni zones boundary [98]. This is coincident with the beginning of the second mercury anomaly [20] and with warming [21], similar to the lowermost Toarcian conditions, although associated with stronger carbon cycle perturbations (figure 1). The belemnite gap could reflect inhospitable conditions in the Lusitanian Basin during the onset of the T-OAE. This might suggest that coleoids—even those with flexible life-history strategies, pre-adapted to such conditions, such as *Ps. longiformis*—could not cope with deteriorating conditions in subtropical epicontinental European basins, resulting in northward migration and/or local extinction during the T-OAE. This would also be consistent with the absence of belemnites in the Riff Mountains during the Levisoni Zone (compare [50,99]).

In fact, the deterioration of water-column conditions must have been worse during the T-OAE in comparison with the Pli–Toa boundary event, namely in terms of oxygenation of the water column, as evidenced by geochemical data [22], and the negative response of marine organisms in the Lusitanian Basin [29]. Moreover, a similar belemnite response was identified in coeval northwest European basins, as the belemnite gap observed in Peniche overlaps with intervals of belemnite gap, or abundant decrease, in the Cleveland, Cardigan Bay and Swabo-Franconian temperate basins. This has been previously interpreted as a response to unfavourable anoxic–euxinic water-column conditions [47,51,100].

Interestingly, the decrease in belemnite abundance, or disappearance, happens before the most severe conditions of the T-OAE are met in subtropical Peniche section (i.e. when the temperature was not the highest, figure 1), and it is not preceded by a body-size decrease. On the contrary, in the Middle and Upper Polymorphum Zone (i.e. from bed P5 to bed P9), belemnite body-size increases at the assemblage scale. However, this might also be partially related to the fact that juveniles become rare due to the unsuitability of habitat. This pattern might indicate that the combination of warming and deoxygenation affected belemnite physiology, reproduction, as well as competition for resources, even before the environmental nadir of the T-OAE. This highlights the importance of climate warming, in addition to regional anoxia, which has been argued to be a major constraint on belemnite abundance and distribution, in the northwest basins of the Tethys Ocean [47,51,100]. However, the widespread anoxia in other parts of the western Tethys (e.g. NW Europe [101]) could have indirectly affected belemnites in the non-anoxic Mediterranean domain (Lusitanian Basin and Morocco) by restricting migratory routes and/or food supply or even by inhibiting their ability to move to cooler refuges, when temperatures began to rise.

Belemnites temporarily re-appear in bed P10 (Upper Levisoni Zone), after the onset of the T-OAE, coinciding, approximately, with the end of the T-OAE-negative CIE (figure 1), with a poor record of *Acrocoelites*. This genus is known to appear and radiate in the northeast basins of the NW Tethys [36,47,48,61,66] after the T-OAE, replacing the genus *Passaloteuthis*, which has been interpreted as an evolutionary adaptation in terms of ecological preferences related to the stressful conditions of the T-OAE [51]. Moreover, the change from the Late Pliensbachian/Early Toarcian Belemnitinae-dominated assemblage to the Middle Toarcian Megateuthidinae-dominated assemblage (together with the disappearance of smaller sized species such as Hastitidae sp. indet., *Parapassaloteuthis* sp. A, *P. milleri*, *Ps. longiformis*), might be related not only to ecological preferences, but also to selective extinction, as pointed out by Payne *et al.* [7], who state that past extinction events were either non-selective, or preferentially removed smaller-bodied taxa. However, the lack of a continuous belemnite record during the Levisoni Zone in Peniche hampers a more detailed assessment. Further research in other basins is necessary to disentangle the extent of this phenomenon.

4.2. The relationship of sedimentary facies to belemnite body-size

Despite the fact that the magnitude of palaeoenvironmental changes relative to the rapid nature of these crisis events [102–104] is quite high on geological timescales [105], their representation in the sedimentary record is influenced by facies evolution. Sedimentary facies depend on several factors such as regional tectonics, climate and sea-level changes, which control the sedimentation rate, which is not constant across the studied interval. We use lithology to account for changes in the facies (related with relative sea-level changes) and belemnite abundance to account for changes in the sedimentation rate, since both are thought to have an effect on morphological patterns [106].

Accumulations with abundant belemnites, particularly observed in beds P4 and P5, could be related to changes in the sedimentation rate relative to the accumulation of belemnites [107]. The lowermost

Polymorphum Zone in Peniche is thought to correspond to a condensed interval [65,91,108]. Our data reveal that belemnite body-size is larger in beds with higher belemnite abundance (electronic supplementary material, figure S10). Abundance, however, does not markedly change across the boundary, where the most significant size change is observed. Regarding lithology, belemnite body-size is larger in marls in comparison with limestones, but these effects are not strong (electronic supplementary material, figure S9).

Our results indicate that when studying the effect of environmental perturbations on belemnite body-size at the scale of the assemblage, lithology and abundance do not affect the pattern observed. Before and after correction, temperature is always the best parameter in explaining the body-size variation. However, the significance is higher without correction, which is not surprising considering that residualizing might also filter out potential ecological signals contained within the sedimentary properties, in addition to the effect of preservation and collection biases. Even with the correction for the effects of sedimentary properties, and despite the existence of a significant model, the analysis failed in revealing a single model to explain belemnite body-size variation. Instead, several models are very similar to the model with the best AICc score. This probably relates to the strong interaction between abiotic parameters, for which we have reasonable proxies when driving body-size patterns during the episodes of climate warming.

However, when analysing the data at species level (*P. bisulcata* and *Ps. longiformis*), the best model for both species in explaining the body-size variation, after correction, is Hg/TOC, as opposed to temperature, without correction. This might be related to the smaller datasets, especially in the case of *P. bisulcata*, which does not allow us to distinguish between individual models. Either way, the increased warming, at the assemblage scale, and Hg/TOC anomalies, as drivers of individual species body-size variation, are not incompatible. They reveal that across the Pli-Toa boundary warming generally correlates with decreasing body-size at the assemblage scale and that the impact of 'catastrophic' environmental perturbations, triggered by volcanism, are the most severe, and probably work in concert, in driving individual species body-size decrease.

The lowermost Toarcian (base of Polymorphum Zone) in Peniche also coincides with a marine transgression [23,65] which might have impacted the size distribution, but differences in lithology and sedimentation rates could not clearly explain size differences in our results. Furthermore, deepening would rather result in finding larger species [76], which would be consistent with our observations of finding larger specimens in marls. However, a body-size decrease is seen across the boundary. Further analyses across different parts of the Lusitanian Basin would be necessary to disentangle the potentially less subtle effects of lithology and sedimentation rates in body-size patterns in shallower sections. As we have no good and/or uncorrelated proxies for other factors such as productivity or ocean acidification, we cannot assess their role in explaining belemnite body-size. However, warming is expected to have impact on all of these environmental parameters.

4.3. Environmental drivers of body-size fluctuations

The Pli–Toa boundary corresponds to the first episode of stress in the Early Toarcian palaeoenvironmental crisis [21], and has been associated with the first pulse of Karoo–Ferrar volcanism [20]. This had a major effect on climate, disturbing the entire ocean–atmosphere system, by causing carbon cycle perturbations, fluctuations in the seawater temperature, widespread deoxygenation and organic matter burial [83]. Our results are consistent with the hypothesis that climate is an important driver of the belemnite body-size variation at the assemblage scale, with a decreasing body-size associated with increasing seawater temperature (electronic supplementary material, figure S8). Salinity could, however, partially affect the interpretation of the oxygen isotopic data, particularly in northwest European basins, where the input of brackish and nutrient-rich Arctic surface waters seems to affect the signal [101,109]. However, decreased salinity has been deemed less significant in Peniche than warming and carbon cycle perturbations, based on phytoplankton communities analyses [30]. Furthermore, modelling suggests that, at these palaeocoordinates, salinity changes are close to zero [101,109], during the studied interval.

The reduction in adult size of *Ps. longiformis* and *P. bisulcata*—the Lilliput effect *sensu stricto*—can potentially be compared with the decrease in adult mantle length of extant squid during rapid warming events [9,11] interpreted to be related to accelerated life histories of squid, with increasing growth rates and shortening lifespans. Individual squid might also require more food per unit body-size, require more oxygen for faster metabolisms and have a reduced capacity to cope without food [77]. To what degree the decrease in adult size relates with direct effects of warming on physiology

(development rate, metabolism and respiration) or instead indirect effects on resource acquisitions, affecting growth and early development, is still under debate [8,110].

Apart from increasing seawater temperature, the mercury anomalies and carbon cycle perturbations at the Pli–Toa boundary event in Peniche, also coincide with increased weathering [22], local decreased productivity [29,30], increasing pCO_2 (and potentially ocean acidification) and decreasing dissolved oxygen [21]. All of these factors are expected to work in concert in driving marine organisms body-size [6], and the results of our analysis of belemnite body-size are consistent with that, especially by the strong collinearity detected between biotic and abiotic parameters (electronic supplementary material, Fig. S4).

Strontium isotopic data from Peniche support the idea of increased weathering during the Pli–Toa boundary warming event, and potentially nutrient influx [22], which is also consistent with the interpretation of enhanced mercury concentration in the sediments. However, counterintuitively, this warming event is interpreted to lead to a decrease in primary productivity, with a decrease in phytoplankton abundance [29,30,45]. This emphasizes how warming and related stressors might affect the size of primary consumers and potentially other levels of the food chain, such as predators like cephalopods. This is also consistent with the increased extinction risk for pelagic predators modelled for various hyperthermal events, including end-Permian mass extinction and the Early Toarcian crisis [7,46]. Additionally, the fact that dwarfing has been observed as a response to starving in laboratorial experiments supports this interpretation [111]. Nonetheless, macroecological studies show that spatial body-size distribution in extant cephalopods is better explained by seawater temperature than productivity [76,112].

The negative CIE observed during the Early Toarcian is interpreted to be related to volcanic outgassing, either directly, by the rapid input of isotopically light carbon into the atmosphere–hydrosphere system [56], or indirectly, by triggering various sources of isotopically light carbon [19]. This would have not only caused rapid climate warming, but also increased pCO_2 and decreased pH of the seawater. Cephalopods are usually interpreted to be quite resistant to ocean acidification in comparison with other marine organisms—cuttlefish even increase calcification. This is interpreted to be related to their strong acid–base regulatory abilities, and to the fact that the cuttlebone is a fully internal structure [113,114]. However, the limited data available hitherto seem to indicate that the effects of acidification might be more severe in early ontogeny, resulting in pathologies [114,115]. Nonetheless, no clear signs of aberrant early development were observed in the studied rostra. More importantly, there are no direct proxies for marked ocean acidification during the Early Toarcian in the Lusitanian Basin and only indirect evidence, such as calcareous nannofossils (*Schizosphaerella*) size reduction. However, this has been interpreted as an indirect consequence of pCO_2 increase, due to the changes in the climate and sea level [29], rather than a direct cause of high pCO_2.

Together with the deposition of organic-rich black shales, the Early Toarcian negative CIE has been traditionally interpreted to reflect increased anoxia in the ocean [82,116]. Irrespective of the potential local or regional overprint of increasing stratification due to basin restriction, or arctic water input, the perturbations at the Pli–Toa boundary event in Peniche are thought to reflect the start of decreasing oxygenation of seawater, while the T-OAE perturbations represent the global peak of anoxia [83]. Nonetheless, there is no evidence for bottom-water anoxia in the Lusitanian Basin [22,117], in contrast with the northwest European basins [118]. Despite that fact, less severe deoxygenation might have played a role in belemnite body-size and distribution, since increased seawater temperature results in reduced oxygen availability relative to demand [119].

The strong collinearity between biotic and abiotic factors available in the literature for the Peniche section (electronic supplementary material, figure S4) hampers an analysis of their individual effect on belemnite body-size. Nonetheless, this study allows investigation of the relationship of belemnite body-size reduction with direct (temperature) and indirect environmental stressors (e.g. deoxygenation, ocean acidification, input of nutrients) associated with climate warming, despite the complex interaction between biotic and abiotic factors, highlighting the importance of taking into account different scales of organization.

5. Conclusion

We document a median body-size decrease of belemnites across the Pli–Toa boundary event, at different scales of palaeobiological organization in the Peniche reference section. We find no evidence for a major taxonomic turnover and the pattern is mainly driven by a decrease in adult size of the dominant taxon

Ps. longiformis—Lilliput effect *sensu stricto*. This phenomenon coincides with the first pulse of the Upper Pliensbachian–Lower Toarcian palaeoenvironmental crisis, probably triggered by volcanism of the Karoo–Ferrar large igneous province. Our results indicate that climate warming best explains the body-size fluctuations observed, although the interplay with perturbations of the carbon cycle, and other environmental factors, possibly triggered by increased volcanogenic outgassing, is evident. Our results suggest that morphological responses precede extinction pulses in belemnites (i.e. during the T-OAE) in the Lusitanian Basin. They also highlight that decreasing adult body-size might rather be a life-history strategy to deal with temporarily deteriorating conditions related to warming, than being a result of taxonomic turnover. During the T-OAE, belemnites disappear from the Lusitanian Basin suggesting their local extinction and/or range shift. Changes within the belemnite assemblage, such as competition and emigration dynamics, seem to play a role in explaining belemnite body-size variation, albeit minor.

References

1. Schmidt DN, Lazarus D, Young JR, Kucera M. 2006 Biogeography and evolution of body size in marine plankton. *Earth Sci. Rev.* **78**, 239–266. (doi:10.1016/j.earscirev.2006.05.004)

2. Daufresne M, Lengfellner K, Sommer U. 2009 Global warming benefits the small in aquatic ecosystems. *Proc. Natl Acad. Sci. USA* **106**, 12 788–12 793. (doi:10.1073/pnas.0902080106)

3. Gardner JL, Peters A, Kearney MR, Joseph L, Heinsohn R. 2011 Declining body size: a third universal response to warming? *Trends Ecol. Evol.* **26**, 285–291. (doi:10.1016/j.tree.2011.03.005)

4. Sheridan JA, Bickford D. 2011 Shrinking body size as an ecological response to climate change. *Nat. Clim. Change* **1**, 401–406. (doi:10.1038/nclimate1259)

5. O'Gorman EJ *et al.* 2017 Unexpected changes in community size structure in a natural warming experiment. *Nat. Clim. Change* **7**, 659–663. (doi:10.1038/nclimate3368)

6. Calosi P, Putnam HM, Twitchett RJ, Vermandele F. 2019 Marine metazoan modern mass extinction: improving predictions by integrating fossil, modern, and physiological data. *Annu. Rev. Mar. Sci.* **11**, 369–390. (doi:10.1146/annurev-marine-010318-095106)

7. Payne JL, Bush AM, Heim NA, Knope ML, McCauley DJ. 2016 Ecological selectivity of the emerging mass extinction in the oceans. *Science* **353**, 1284–1286. (doi:10.1126/science.aaf2416)

8. Ohlberger J. 2013 Climate warming and ectotherm body size—from individual physiology to community ecology. *Funct. Ecol.* **27**, 991–1001. (doi:10.1111/1365-2435.12098)

9. Hoving HJ *et al.* 2013 Extreme plasticity in life-history strategy allows a migratory predator (jumbo squid) to cope with a changing climate. *Glob. Change Biol.* **19**, 2089–2103. (doi:10.1111/gcb.12198)

10. Moreno A, Azevedo M, Pereira J, Pierce GJ. 2007 Growth strategies in the squid *Loligo vulgaris* from Portuguese waters. *Mar. Biol. Res.* **3**, 49–59. (doi:10.1080/17451000601129115)

11. Jackson GD, Domeier ML. 2003 The effects of an extraordinary El Niño/La Niña event on the size and growth of the squid *Loligo opalescens* off Southern California. *Mar. Biol.* **142**, 925–935. (doi:10.1007/s00227-002-1005-4)

12. Urbanek A. 1993 Biotic crises in the history of Upper Silurian graptoloids: a palaeobiological model. *Hist. Biol.* **7**, 29–50. (doi:10.1080/10292389309380442)

13. Twitchett RJ. 2007 The Lilliput effect in the aftermath of the end-Permian extinction event. *Palaeogeogr. Palaeoclimatol. Palaeoecol.* **252**, 132–144. (doi:10.1016/j.palaeo.2006.11.038)

14. Harries PJ, Knorr PO. 2009 What does the 'Lilliput Effect' mean? *Palaeogeogr. Palaeoclimatol. Palaeoecol.* **284**, 4–10. (doi:10.1016/j.palaeo.2009.08.021)

15. Morten SD, Twitchett RJ. 2009 Fluctuations in the body size of marine invertebrates through the Pliensbachian–Toarcian extinction event. *Palaeogeogr. Palaeoclimatol. Palaeoecol.* **284**, 29–38. (doi:10.1016/j.palaeo.2009.08.023)

16. Danise S, Twitchett RJ, Little CTS, Clémence M-E. 2013 The impact of global warming and anoxia on marine benthic community dynamics: an example from the Toarcian (Early Jurassic). *PLoS ONE* **8**, e56255. (doi:10.1371/journal.pone.0056255)

17. Caruthers AH, Smith PL, Gröcke DR. 2013 The Pliensbachian–Toarcian (Early Jurassic) extinction, a global multi-phased event. *Palaeogeogr. Palaeoclimatol. Palaeoecol.* **386**, 104–118. (doi:10.1016/j.palaeo.2013.05.010)

18. Ogg JG, Ogg GM, Gradstein FM. 2016 Jurassic. In *A concise geologic time scale* (eds JG Ogg, GM Ogg, FM Gradstein), pp. 151–166. Amsterdam, The Netherlands: Elsevier.

19. Ruebsam W, Mayer B, Schwark L. 2019 Cryosphere carbon dynamics control early Toarcian global warming and sea level evolution. *Glob. Planet. Change* **172**, 440–453. (doi:10.1016/j.gloplacha.2018.11.003)

20. Percival LME *et al.* 2015 Globally enhanced mercury deposition during the end-Pliensbachian extinction and Toarcian OAE: a link to the Karoo–Ferrar Large Igneous Province.

Earth Planet. Sci. Lett. **428**, 267–280. (doi:10.1016/j.epsl.2015.06.064)

21. Suan G, Mattioli E, Pittet B, Mailliot S, Lécuyer C. 2008 Evidence for major environmental perturbation prior to and during the Toarcian (Early Jurassic) oceanic anoxic event from the Lusitanian Basin, Portugal. *Paleoceanography* **23**, A1202. (doi:10.1029/2007PA001459)

22. Hesselbo SP, Jenkyns HC, Duarte LV, Oliveira LCV. 2007 Carbon-isotope record of the Early Jurassic (Toarcian) Oceanic Anoxic Event from fossil wood and marine carbonate (Lusitanian Basin, Portugal). *Earth Planet. Sci. Lett.* **253**, 455–470. (doi:10.1016/j.epsl.2006.11.009)

23. Duarte LV. 2007 Lithostratigraphy, sequence stratigraphy and depositional setting of the Pliensbachian and Toarcian series in the Lusitanian Basin (Portugal). In *The Peniche Section (Portugal) contributions to the definition of the Toarcian GSSP: International Subcommission on Jurassic Stratigraphy* (ed. RB Rocha), pp. 17–23.

24. Korte C, Hesselbo SP. 2011 Shallow marine carbon and oxygen isotope and elemental records indicate icehouse-greenhouse cycles during the Early Jurassic. *Paleoceanography* **26**, PA4219. (doi:10.1029/2011PA002160)

25. Rosales I, Quesada S, Robles S. 2004 Paleotemperature variations of Early Jurassic seawater recorded in geochemical trends of belemnites from the Basque–Cantabrian basin, northern Spain. *Palaeogeogr. Palaeoclimatol. Palaeoecol.* **203**, 253–275. (doi:10.1016/S0031-0182(03)00686-2)

26. Rosales I, Barnolas A, Goy A, Sevillano A, Armendáriz M, López-García JM. 2018 Isotope records (C-O-Sr) of late Pliensbachian-early Toarcian environmental perturbations in the westernmost Tethys (Majorca Island, Spain). *Palaeogeogr. Palaeoclimatol. Palaeoecol.* **497**, 168–185. (doi:10.1016/j.palaeo.2018.02.016)

27. Suan G, Mattioli E, Pittet B, Lécuyer C, Suchéras-Marx B, Duarte LV, Philippe M, Reggiani L, Martineau F. 2010 Secular environmental precursors to Early Toarcian (Jurassic) extreme climate changes. *Earth Planet. Sci. Lett.* **290**, 448–458. (doi:10.1016/j.epsl.2009.12.047)

28. Littler K, Hesselbo SP, Jenkyns HC. 2010 A carbon-isotope perturbation at the Pliensbachian–Toarcian boundary: evidence from the Lias Group, NE England. *Geol. Mag.* **147**, 181–192. (doi:10.1017/S0016756809990458)

29. Mattioli E, Pittet B, Petitpierre L, Mailliot S. 2009 Dramatic decrease of pelagic carbonate production by nannoplankton across the Early Toarcian anoxic event (T-OAE). *Glob. Planet. Change* **65**, 134–145. (doi:10.1016/j.gloplacha.2008.10.018)

30. Correia VF, Riding JB, Duarte LV, Fernandes P, Pereira Z. 2017 The palynological response to the Toarcian Oceanic Anoxic Event (Early Jurassic) at Peniche, Lusitanian Basin, western Portugal. *Mar. Micropaleontol.* **137**, 46–63. (doi:10.1016/j.marmicro.2017.10.004)

31. Aberhan M, Fürsich FT. 1996 Diversity analysis of Lower Jurassic bivalves of the Andean Basin

and the Pliensbachian-Toarcian mass extinction. *Lethaia* **29**, 181–195. (doi:10.1111/j.1502-3931.1996.tb01874.x)

32. Dera G, Neige P, Dommergues J-L, Fara E, Laffont R, Pellenard P. 2010 High-resolution dynamics of Early Jurassic marine extinctions: the case of Pliensbachian–Toarcian ammonites (Cephalopoda). *J. Geol. Soc.* **167**, 21–33. (doi:10.1144/0016-76492009-068)

33. Little CT. 1995 The Pliensbachian-Toarcian (Lower Jurassic) extinction event. Doctoral dissertation, University of Bristol.

34. Caswell BA, Coe AL, Cohen AS. 2009 New range data for marine invertebrate species across the early Toarcian (Early Jurassic) mass extinction. *J. Geol. Soc.* **166**, 859–872. (doi:10.1144/0016-76492008-0831)

35. Schlegelmilch R. 1998 *Die belemniten des süddeutschen Jura*, 151 p. Stuttgart, Germany: Gustav Fischer.

36. Weis R, Neige P, Dugué O, Cencio AD, Thuy B, Numberger-Thuy L, Mariotti N. 2018 Lower Jurassic (Pliensbachian-Toarcian) belemnites from Fresney-le-Puceux (Calvados, France): taxonomy, chronostratigraphy and diversity. *Geodiversitas* **40**, 87–113. (doi:10.5252/geodiversitas2018v40a4)

37. Gómez J, Comas-Rengifo M, Goy A. 2015 Palaeoclimatic oscillations in the Pliensbachian (Lower Jurassic) of the Asturian Basin (Northern Spain). *Clim. Past Discussions* **11**, 4039–4076. (doi:10.5194/cpd-11-4039-2015)

38. Hesselbo SP, Grocke DR, Jenkyns HC, Bjerrum CJ, Farrimond P, Morgans Bell HS, Green OR. 2000 Massive dissociation of gas hydrate during a Jurassic oceanic anoxic event. *Nature* **406**, 392–395. (doi:10.1038/35019044)

39. Jenkyns HC. 1988 The early Toarcian (Jurassic) anoxic event; stratigraphic, sedimentary and geochemical evidence. *Am. J. Sci.* **288**, 101–151. (doi:10.2475/ajs.288.2.101)

40. Wignall PB, Newton RJ, Little CT. 2005 The timing of paleoenvironmental change and cause-and-effect relationships during the Early Jurassic mass extinction in Europe. *Am. J. Sci.* **305**, 1014–1032. (doi:10.2475/ajs.305.10.1014)

41. Cecca F, Macchioni F. 2004 The two Early Toarcian (Early Jurassic) extinction events in ammonoids. *Lethaia* **37**, 35–56. (doi:10.1080/00241160310008257)

42. Little CTS, Benton MJ. 1995 Early Jurassic mass extinction: a global long-term event. *Geology* **23**, 495–498. (doi:10.1130/0091-7613(1995)023<0495:EJMEAG>2.3.CO;2)

43. Harries PJ, Little CTS. 1999 The early Toarcian (Early Jurassic) and the Cenomanian–Turonian (Late Cretaceous) mass extinctions: similarities and contrasts. *Palaeogeogr. Palaeoclimatol. Palaeoecol.* **154**, 39–66. (doi:10.1016/S0031-0182(99)00086-3)

44. García Joral F, Gómez JJ, Goy A. 2011 Mass extinction and recovery of the Early Toarcian (Early Jurassic) brachiopods linked to climate change in Northern and Central Spain. *Palaeogeogr. Palaeoclimatol. Palaeoecol.* **302**, 367–380. (doi:10.1016/j.palaeo.2011.01.023)

45. Caswell BA, Coe AL. 2013 Primary productivity controls on opportunistic bivalves during Early

Jurassic oceanic deoxygenation. *Geology* **41**, 1163–1166. (doi:10.1130/G34819.1)

46. Dunhill AM, Foster WJ, Azaele S, Sciberras J, Twitchett RJ. 2018 Modelling determinants of extinction across two Mesozoic hyperthermal events. *Proc. R. Soc. B* **285**, 20180404. (doi:10.1098/rspb.2018.0404)

47. Caswell BA, Coe AL. 2014 The impact of anoxia on pelagic macrofauna during the Toarcian Oceanic Anoxic Event (Early Jurassic). *Proc. Geol. Assoc.* **125**, 383–391. (doi:10.1016/j.pgeola.2014.06.001)

48. Dera G, Toumoulin A, De Baets K. 2016 Diversity and morphological evolution of Jurassic belemnites from South Germany. *Palaeogeogr. Palaeoclimatol. Palaeoecol.* **457**, 80–97. (doi:10.1016/j.palaeo.2016.05.029)

49. Doyle P. 1987 Lower Jurassic-Lower Cretaceous belemnite biogeography and the development of the Mesozoic Boreal Realm. *Palaeogeogr. Palaeoclimatol. Palaeoecol.* **61**, 237–254. (doi:10.1016/0031-0182(87)90052-6)

50. Sanders MT, Bardin J, Benzaggagh M, Cecca F. 2015 Early Toarcian (Jurassic) belemnites from northeastern Gondwana (South Riffian ridges, Morocco). *Paläontol. Z.* **89**, 51–62. (doi:10.1007/s12542-013-0214-0)

51. Ullmann CV, Thibault N, Ruhl M, Hesselbo SP, Korte C. 2014 Effect of a Jurassic oceanic anoxic event on belemnite ecology and evolution. *Proc. Natl Acad. Sci. USA* **111**, 10 073–10 076. (doi:10.1073/pnas.1320156111)

52. Jenkyns HC, Clayton CJ. 1986 Black shales and carbon isotopes in pelagic sediments from the Tethyan Lower Jurassic. *Sedimentology* **33**, 87–106. (doi:10.1111/j.1365-3091.1986.tb00746.x)

53. Jenkyns HC, Clayton CJ. 1997 Lower Jurassic epicontinental carbonates and mudstones from England and Wales: chemostratigraphic signals and the early Toarcian anoxic event. *Sedimentology* **44**, 687–706. (doi:10.1046/j.1365-3091.1997.d01-43.x)

54. Hermoso M, Le Callonnec L, Minoletti F, Renard M, Hesselbo SP. 2009 Expression of the Early Toarcian negative carbon-isotope excursion in separated carbonate microfractions (Jurassic, Paris Basin). *Earth Planet. Sci. Lett.* **277**, 194–203. (doi:10.1016/j.epsl.2008.10.013)

55. Them TR, Jagoe CH, Caruthers AH, Gill BC, Grasby SE, Gröcke DR, Yin R, Owens JD. 2019 Terrestrial sources as the primary delivery mechanism of mercury to the oceans across the Toarcian Oceanic Anoxic Event (Early Jurassic). *Earth Planet. Sci. Lett.* **507**, 62–72. (doi:10.1016/j.epsl.2018.11.029)

56. Pálfy JZ, Smith PL. 2000 Synchrony between Early Jurassic extinction, oceanic anoxic event, and the Karoo-Ferrar flood basalt volcanism. *Geology* **28**, 747–750. (doi:10.1130/0091-7613(2000)28<747:SBEJEO>2.0.CO;2)

57. Moore JK et al. 2018 Sustained climate warming drives declining marine biological productivity. *Science* **359**, 1139–1143. (doi:10.1126/science.aao6379)

58. Caswell BA, Paine M, Frid CLJ. 2018 Seafloor ecological functioning over two decades of organic enrichment. *Mar. Pollut. Bull.* **136**, 212–229. (doi:10.1016/j.marpolbul.2018.08.041)

59. Wilson J, Monteiro F, Schmidt D, Ward B, Ridgwell A. 2018 Linking marine plankton ecosystems and climate: a new modeling approach to the warm early Eocene climate. *Paleoceanogr. Paleoclimatol.* **33**, 1439–1452. (doi:10.1029/2018PA003374)

60. Ilyina T, Heinze M. 2019 Carbonate dissolution enhanced by ocean stagnation and respiration at the onset of the Paleocene-Eocene thermal maximum. *Geophys. Res. Lett.* **46**, 842–852. (doi:10.1029/2018GL080761)

61. Doyle P. 1990 The British Toarcian (lower Jurassic) belemnites: part 1. *Monogr. Palaeontogr. Soc.* **584**, 1–49.

62. Harazim D, Van De Schootbrugge BAS, Sorichter K, Fiebig J, Weug A, Suan G, Oschmann W. 2013 Spatial variability of watermass conditions within the European Epicontinental Seaway during the Early Jurassic (Pliensbachian–Toarcian). *Sedimentology* **60**, 359–390. (doi:10.1111/j.1365-3091.2012.01344.x)

63. McArthur J, Doyle P, Leng M, Reeves K, Williams C, Garcia-Sanchez R, Howarth RJ. 2007 Testing palaeo-environmental proxies in Jurassic belemnites: Mg/Ca, Sr/Ca, Na/Ca, δ^{18}O and δ^{13}C. *Palaeogeogr. Palaeoclimatol. Palaeoecol.* **252**, 464–480. (doi:10.1016/j.palaeo.2007.05.006)

64. van de Schootbrugge B, McArthur JM, Bailey TR, Rosenthal Y, Wright JD, Miller KG. 2005 Toarcian oceanic anoxic event: an assessment of global causes using belemnite C isotope records. *Paleoceanography* **20**, A3008. (doi:10.1029/2004PA001102)

65. Rocha RB et al. 2016 Base of the Toarcian stage of the lower Jurassic defined by the global boundary stratotype section and point (GSSP) at the Peniche section (Portugal). *Episodes J. Int. Geosci.* **39**, 460–481. (doi:10.18814/epiiugs/2016/v39i3/99741)

66. Doyle P. 1992 The British Toarcian (lower Jurassic) belemnites: part 2. *Monogr. Palaeontogr. Soc.* **587**, 50–79.

67. Pinard J-D, Weis R, Neige P, Mariotti N, Di Cencio A. 2014 Belemnites from the Upper Pliensbachian and the Toarcian (Lower Jurassic) of Tournadous (Causses, France). *Neues Jahrb. Geol. Paläont.-Abhandlungen* **273**, 155–177. (doi:10.1127/0077-7749/2014/0421)

68. Tomašových A, Schlögl J, Biroň A, Hudáčková N, Mikuš T. 2017 Taphonomic clock and bathymetric dependence of cephalopod preservation in bathyal, sediment-starved environments. *PALAIOS* **32**, 135–152. (doi:10.2110/palo.2016.039)

69. Rita P, De Baets K, Schlott M. 2018 Rostrum size differences between Toarcian belemnite battlefields. *Fossil Record.* **21**, 171–182. (doi:10.5194/fr-21-171-2018)

70. Monks N, Hardwick JD, Gale AS. 1996 The function of the belemnite guard. *Paläontol. Z.* **70**, 425. (doi:10.1007/BF02988082)

71. Benito MI, Reolid M, Viedma C. 2016 On the microstructure, growth pattern and original porosity of belemnite rostra: insights from calcitic Jurassic belemnites. *J. Iber. Geol.* **42**, 201.

72. Hoffmann R, Richter DK, Neuser RD, Jöns N, Linzmeier BJ, Lemanis RE, Fusseis F, Xiao X, Immenhauser A. 2016 Evidence for a composite organic–inorganic fabric of belemnite rostra: implications for palaeoceanography and palaeoecology. *Sediment. Geol.* **341**, 203–215. (doi:10.1016/j.sedgeo.2016.06.001)

73. Reitner J, Urlichs M. 1983 Echte Weichteilbelemniten aus dem Untertoarcium (Posidonienschiefer) Südwestdeutschlands. *Neues Jahrb. Geol. Paläontol.* **165**, 450–465.

74. Klug C, Schweigert G, Fuchs D, Kruta I, Tischlinger H. 2016 Adaptations to squid-style high-speed swimming in Jurassic belemnitids. *Biol. Lett.* **12**, 20150877. (doi:10.1098/rsbl.2015.0877)

75. Jenny D, Fuchs D, Arkhipkin AI, Hauff RB, Fritschi B, Klug C. 2019 Predatory behaviour and taphonomy of a Jurassic belemnoid coleoid (Diplobelida, Cephalopoda). *Sci. Rep.* **9**, 7944. (doi:10.1038/s41598-019-44260-w)

76. Rosa R, Gonzalez L, Dierssen HM, Seibel BA. 2012 Environmental determinants of latitudinal size-trends in cephalopods. *Mar. Ecol. Prog. Ser.* **464**, 153–165. (doi:10.3354/meps09822)

77. Pecl GT, Jackson GD. 2008 The potential impacts of climate change on inshore squid: biology, ecology and fisheries. *Rev. Fish Biol. Fish.* **18**, 373–385. (doi:10.1007/s11160-007-9077-3)

78. Rego BL, Wang SC, Altiner D, Payne JL. 2012 Within- and among-genus components of size evolution during mass extinction, recovery, and background intervals: a case study of Late Permian through Late Triassic foraminifera. *Paleobiology* **38**, 627–643. (doi:10.1666/11040.1)

79. Oksanen J et al. 2018 Vegan: community ecology package. R package version 2.5-2. See https://CRAN.R-project.org/package=vegan.

80. R Development Core Team. 2018 *R: a language and environment for statistical computing*. Vienna, Austria: R Foundation for Statistical Computing. Retrieved from http://www.R-project.org.

81. Cárdenas AL, Harries PJ. 2010 Effect of nutrient availability on marine origination rates throughout the Phanerozoic eon. *Nat. Geosci.* **3**, 430. (doi:10.1038/ngeo869)

82. Jenkyns HC. 2010 Geochemistry of oceanic anoxic events. *Geochem. Geophys. Geosyst.* **11**. (doi:10.1029/2009GC002788)

83. Them TR et al. 2018 Thallium isotopes reveal protracted anoxia during the Toarcian (Early Jurassic) associated with volcanism, carbon burial, and mass extinction. *Proc. Natl Acad. Sci. USA* **115**, 6596–6601. (doi:10.1073/pnas.1803478115)

84. Jakob EM, Marshall SD, Uetz GW. 1996 Estimating fitness: a comparison of body condition indices. *Oikos* **77**, 61–67. (doi:10.2307/3545585)

85. Box GEP, Jenkins GM, Reinsel GC. 1994 *Time series analysis: forecasting and control*. Upper Saddle River, NJ: Prentice Hall.

86. Pinheiro J, Bates D, DebRoy S, Sarkar D, R Core Team. 2018 nlme: linear and nonlinear mixed effects models. R package version 3.1-137. See https://CRAN.R-project.org/package=nlme.

87. Spiess A-N. 2018 qpcR: modelling and analysis of real-time PCR data. R package version 1.4-1. See https://cran.R-project.org/web/packages/qpcR/.

88. Arkhipkin A, Weis R, Mariotti N, Shcherbich Z. 2015 'Tailed' cephalopods. *J. Mollusc. Stud.* **81**, 345–355. (doi:10.1093/mollus/eyu094)

89. Doyle P. 1985 Sexual dimorphism in the belemnite Youngibelus from the Lower Jurassic of Yorkshire. *Palaeontology* **28**, 133–146.

90. Comas-Rengifo MJ, Duarte LV, Felix FF, Joral FG, Goy A, Rocha RB. 2015 Latest Pliensbachian-Early Toarcian brachiopod assemblages from the Peniche section (Portugal) and their correlation. *Episodes* **38**, 2–8. (doi:10.18814/epiiugs/2015/v38i1/001)

91. Rita P, Reolid M, Duarte LV. 2016 Benthic foraminiferal assemblages record major environmental perturbations during the Late Pliensbachian–Early Toarcian interval in the Peniche GSSP, Portugal. *Palaeogeogr. Palaeoclimatol. Palaeoecol.* **454**, 267–281. (doi:10.1016/j.palaeo.2016.04.039)

92. Reolid M, Duarte LV, Rita P. 2019 Changes in foraminiferal assemblages and environmental conditions during the T-OAE (Early Jurassic) in the northern Lusitanian Basin, Portugal. *Palaeogeogr. Palaeoclimatol. Palaeoecol.* **520**, 30–43. (doi:10.1016/j.palaeo.2019.01.022)

93. Pauly D. 1980 On the interrelationships between natural mortality, growth parameters, and mean environmental temperature in 175 fish stocks. *ICES J. Mar. Sci.* **39**, 175–192. (doi:10.1093/icesjms/39.2.175)

94. Audzijonyte A, Richards SA. 2018 The energetic cost of reproduction and its effect on optimal life-history strategies. *Am. Nat.* **192**, E150–E162. (doi:10.1086/698655)

95. Neige P, Boletzky SV. 1997 Morphometrics of the shell of three Sepia species (Mollusca: Cephalopoda): intra-and interspecific variation. *Zool. Beitr.* **38**, 137–156.

96. Poloczanska ES et al. 2013 Global imprint of climate change on marine life. *Nat. Clim. Change* **3**, 919. (doi:10.1038/nclimate1958)

97. Reddin CJ, Kocsis ÁT, Kiessling W. 2018 Marine invertebrate migrations trace climate change over 450 million years. *Glob. Ecol. Biogeogr.* **27**, 704–713. (doi:10.1111/geb.12732)

98. Duarte LV et al. 2018 The Toarcian Oceanic Anoxic Event at Peniche. An exercise in integrated stratigraphy—Stop 1.3. In *Field trip Guidebook: The Toarcian Oceanic Anoxic Event in the Western Iberian Margin and its context within the Lower Jurassic evolution of the Lusitanian Basin*, p. 54. Coimbra, Portugal: University of Coimbra.

99. Bardin J, Rouget I, Benzaggagh M, Fürsich FT, Cecca F. 2015 Lower Toarcian (Jurassic) ammonites of the South Riffian ridges (Morocco): systematics and biostratigraphy. *J. Syst. Paleontol.* **13**, 471–501. (doi:10.1080/14772019.2014.937204)

100. Xu W et al. 2018 Evolution of the Toarcian (Early Jurassic) carbon-cycle and global climatic controls on local sedimentary processes (Cardigan Bay Basin. UK). *Earth Planet. Sci. Lett.* **484**, 396–411. (doi:10.1016/j.epsl.2017.12.037)

101. Ruvalcaba Baroni I et al. 2018 Ocean circulation in the Toarcian (Early Jurassic): a key control on deoxygenation and carbon burial on the European Shelf. *Paleoceanogr. Paleoclimatol.* **33**, 994–1012. (doi:10.1029/2018PA003394)

102. Boulila S, Galbrun B, Sadki D, Gardin S, Bartolini A. 2019 Constraints on the duration of the early Toarcian T-OAE and evidence for carbon-reservoir change from the High Atlas (Morocco). *Glob. Planet. Change* **175**, 113–128. (doi:10. 1016/j.gloplacha.2019.02.005)

103. Huang C, Hesselbo SP. 2014 Pacing of the Toarcian Oceanic Anoxic Event (Early Jurassic) from astronomical correlation of marine sections. *Gondwana Res.* **25**, 1348–1356. (doi:10.1016/j.gr.2013.06.023)

104. Suan G, Pittet B, Bour I, Mattioli E, Duarte LV, Mailliot S. 2008 Duration of the Early Toarcian carbon isotope excursion deduced from spectral analysis: consequence for its possible causes. *Earth Planet. Sci. Lett.* **267**, 666–679. (doi:10. 1016/j.epsl.2007.12.017)

105. Kemp DB, Eichenseer K, Kiessling W. 2015 Maximum rates of climate change are systematically underestimated in the geological record. *Nat. Commun.* **6**, 8890. (doi:10.1038/ncomms9890)

106. Holland SM. 2000 The quality of the fossil record: a sequence stratigraphic perspective. *Paleobiology* **26**, 148–168. (doi:10.1017/S0094837300026919)

107. Doyle P, Macdonald DI. 1993 Belemnite battlefields. *Lethaia* **26**, 65–80. (doi:10.1111/j. 1502-3931.1993.tb01513.x)

108. Pittet B, Suan G, Lenoir F, Duarte LV, Mattioli E. 2014 Carbon isotope evidence for sedimentary discontinuities in the lower Toarcian of the Lusitanian Basin (Portugal): sea level change at the onset of the Oceanic Anoxic Event. *Sediment. Geol.* **303**, 1–14. (doi:10.1016/j. sedgeo.2014.01.001)

109. Dera G, Donnadieu Y. 2012 Modeling evidences for global warming, Arctic seawater freshening, and sluggish oceanic circulation during the Early Toarcian anoxic event. *Paleoceanogr. Paleoclimatol.* **27**, PA2211.

110. Audzijonyte A, Barneche DR, Baudron AR, Belmaker J, Clark TD, Marshall CT, Morrongiello JR, Van Rijn I. 2019 Is oxygen limitation in warming waters a valid mechanism to explain decreased body sizes in aquatic ectotherms? *Global Ecol. Biogeogr.* **28**, 64–77. (doi:10.1111/geb.12847)

111. Boletzky SV. 1974 Effets de la sous-nutrition prolongée sur le développement de la coquille de *Sepia officinalis* L. (Mollusca, Cephalopoda). *Bull. Soc. Zool. France* **99**, 667–673.

112. Pauly D, Kinne O. 2010 *Gasping fish and panting squids: oxygen, temperature and the growth of water-breathing animals*. Oldendorf/Luhe, Germany: International Ecology Institute.

113. Gutowska MA, Melzner F, Pörtner HO, Meier S. 2010 Cuttlebone calcification increases during exposure to elevated seawater pCO_2 in the cephalopod *Sepia officinalis*. *Mar. Biol.* **157**, 1653–1663. (doi:10.1007/s00227-010-1438-0)

114. Dorey N, Melzner F, Martin S, Oberhänsli F, Teyssié J-L, Bustamante P, Gattuso J-P, Lacoue-Labarthe T. 2013 Ocean acidification and temperature rise: effects on calcification during early development of the cuttlefish *Sepia officinalis*. *Mar. Biol.* **160**, 2007–2022. (doi:10. 1007/s00227-012-2059-6)

115. Lacoue-Labarthe T, Reveillac E, Oberhänsli F, Teyssié J-L, Jeffree R, Gattuso J. 2011 Effects of ocean acidification on trace element accumulation in the early-life stages of squid *Loligo vulgaris*. *Aquat. Toxicol.* **105**, 166–176. (doi:10.1016/j.aquatox.2011.05.021)

116. Ikeda M, Hori RS, Ikehara M, Miyashita R, Chino M, Yamada K. 2018 Carbon cycle dynamics linked with Karoo-Ferrar volcanism and astronomical cycles during Pliensbachian-Toarcian (Early Jurassic). *Glob. Planet. Change* **170**, 163–171. (doi:10.1016/j.gloplacha.2018. 08.012)

117. Rodríguez-Tovar FJ, Miguez-Salas O, Duarte LV. 2017 Toarcian Oceanic Anoxic Event induced unusual behaviour and palaeobiological changes in *Thalassinoides* tracemakers. *Palaeogeogr. Palaeoclimatol. Palaeoecol.* **485**, 46–56. (doi:10.1016/j.palaeo.2017. 06.002)

118. McArthur JM, Algeo TJ, van de Schootbrugge B, Li Q, Howarth RJ. 2008 Basinal restriction, black shales, Re-Os dating, and the Early Toarcian (Jurassic) oceanic anoxic event. *Paleoceanography* **23**, PA4217. (doi:10.1029/2008PA001607)

119. Verberk WCEP, Atkinson D. 2013 Why polar gigantism and Palaeozoic gigantism are not equivalent: effects of oxygen and temperature on the body size of ectotherms. *Funct. Ecol.* **27**, 1275–1285. (doi:10.1111/1365-2435.12152)